#3930

Natural Convection in Undivided and Partially Divided Rectangular Enclosures

M. W. Nansteel

R. Greif
Mem. ASME

Passive Solar Analysis and Design Group, Lawrence Berkeley Laboratory and Department of Mechanical Engineering, University of California, Berkeley, Calif. 94720

Heat transfer by natural convection in a two-dimensional rectangular enclosure fitted with partial vertical divisions is investigated experimentally. The horizontal walls of the enclosure are adiabatic while the vertical walls are maintained at different temperatures. The experiments are carried out with water, $Pr \simeq 3.5$, for Rayleigh numbers in the range, $2.3 \times 10^{10} \leq Ra_L \leq 1.1 \times 10^{11}$, and an aspect ratio, $A = H/L = \frac{1}{2}$. The effect of the partial vertical divisions on the fluid flow and temperature fields is investigated by dye-injection flow visualization and by thermocouple probes, respectively. The effect of the partitions on the heat transfer across the enclosure is also studied and correlations for the Nusselt number as a function of Ra_L and partition length are generated for both conducting and non-conducting partition materials. Partial divisions are found to have a significant effect on the heat transfer; especially when the divisions are adiabatic. The results also indicate that the partial divisions may have a stabilizing effect on the laminar-transitional flow on the heated vertical walls of the enclosure.

Introduction

Natural convection heat transfer in rectangular enclosures is of great importance in determining the energy transfer within buildings, especially those incorporating passive solar design features. This configuration has been studied extensively, e.g., [1–19, 25], but only for limited ranges of the Rayleigh number. The effect of a partial obstruction extending downward from the enclosure ceiling is also of importance but has received little attention [cf. 17, 20–24]. This geometry corresponds roughly, for example, to a ceiling beam or soffit. The experimental investigation of Duxbury [20] was carried out in rectangular enclosures of aspect ratios (see Fig. 1), $\frac{2}{3} \leq A = H/L \leq 5$, partially divided by vertical, heat conducting partitions using air as the working fluid, for Rayleigh numbers approaching 10^6. The driving force in Duxbury's experiment was the imposed temperature difference between the two vertical sidewalls of the enclosure. The experiments and numerical calculations of Lloyd, et al. [21, 22] were motivated by fire studies and there the flow was driven by methane combustion and by surface or volumetric heat sources. The experimental and numerical study of Bauman, et al. [17] was motivated by studies of heat transfer within buildings and focused on the undivided enclosure although some results are also presented for a partially divided enclosure. This study [17] was carried out in water in a partially divided rectangular enclosure of aspect ratio, $A = \frac{1}{2}$ and $Ra_L \sim 10^{10}$. Janikowski, et al. [23] experimentally investigated the temperature and flow fields inside a rectangular enclosure partially divided by solid and porous vertical divisions extending upward from the floor and downward from the ceiling simultaneously. Emery [24], on the other hand, studied the heat transfer and temperature field in a rectangular enclosure fitted with a vertical partial division extending from the center of the enclosure downward toward the floor and upward toward the ceiling. It appears, however, that there has not been any thorough investigation of the role played by partial vertical divisions at the high values of the Rayleigh number ($Ra_L \sim 10^{10} - 10^{12}$) that are commonly encountered.

The primary goal of this study is to develop, through careful experiments, an understanding of the convective heat transfer processes and fluid flow occurring in the two-dimensional, partially divided enclosure (see Fig. 1) at Rayleigh numbers representative of large scale applications. An immediate application is in convection analyses in passive solar heated buildings. The experiment is carried out in a rectangular enclosure of aspect ratio, $A = H/L = \frac{1}{2}$, with isothermal vertical sidewalls and insulated horizontal floor and ceiling. The enclosure is fitted with either thermally conducting or non-conducting vertical partitions of various lengths (aperture ratios, $A_p = h/H = 1$ (no partition), $\frac{3}{4}$, $\frac{1}{2}$ and $\frac{1}{4}$ are investigated). Experiments are carried out with water ($3 \leq Pr \leq 4.3$) as the working fluid at Rayleigh numbers over the range $2.3 \times 10^{10} \leq Ra_L \leq 1.1 \times 10^{11}$.

It is emphasized that over this Rayleigh number range the results without the partition are also new. Power law correlations are obtained giving the dependence of the Nusselt number on aperture ratio, Rayleigh number, and partition conductance. Temperature profiles are also obtained within the enclosure with thermocouple probes, and the basic flow structure is noted by using dye-injection flow visualization. Distinct differences are found between the flow pattern observed in these experiments and those observed in the lower Ra_L and lower Pr experiments of Duxbury. Also, the presence of laminar-transitional flow for $A_p = 1$ (no partition) and the suppression of transition for $A_p < 1$ are discussed.

Experimental Apparatus and Procedure

The experimental apparatus consisted basically of a rectangular enclosure of height, $H = 15.2$ cm, width, $L = 30.5$ cm (aspect ratio, $A = H/L = \frac{1}{2}$) and breadth, $B = 83.8$ cm. This system is similar to the one used by Bauman, et al. [17]. The heated and cooled vertical walls

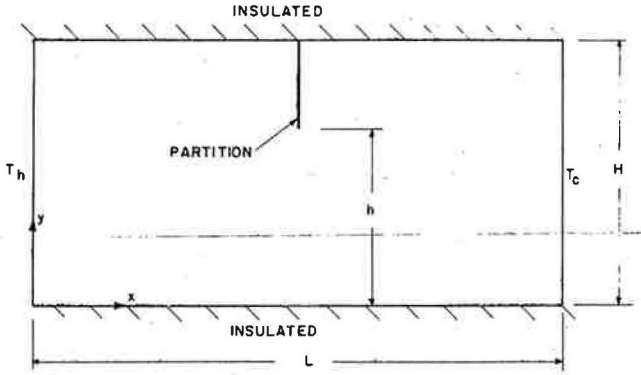

Fig. 1 Rectangular enclosure with partial vertical division

Contributed by the Heat Transfer Division for publication in the JOURNAL OF HEAT TRANSFER. Manuscript received by the Heat Transfer Division July 27, 1981.

were made from plates of copper, 4.8 mm thick, and aluminum, 15.9 mm thick, respectively, while the floor, ceiling, and endwalls of the enclosure were fabricated from clear, 1.27 cm thick plexiglas. The copper hot wall was heated electrically with 18 Minco "Thermofoil" resistance heaters. These were arranged in three vertical columns of six heaters each, see Fig. 2. In order to limit temperature variations along the hot wall, in the vertical direction, each pair of heaters in a given column was supplied by a separate 120V/240V a–c power supply. In this way, hot wall temperature deviations from the average hot wall temperature were kept to within about 10 percent of the overall temperature difference across the enclosure ($T_h - T_c$). The aluminum cold wall was cooled by passing tap water through two rectangular channels which were machined into the aluminum cold plate, traversing the full breadth of the enclosure seven times. It was found that temperature variations along the cold wall could be kept below about 10 percent of the temperature difference ($T_h - T_c$) by using a sufficiently high cooling water flow rate. Two streams entered the aluminum manifold near the top of the cold wall and were extracted near the bottom, see Fig. 2.

Joints between the copper and aluminum vertical walls and plexiglas floor were sealed with a 1.6 mm thick cork gasket to minimize conduction between the vertical surfaces and the floor. The ceiling was removable and was thermally isolated from the hot and cold walls by a small air gap, as in Fig. 2.

Partial vertical divisions of lengths 0, 3.8, 7.6 and 11.4 cm, extended downward from the center of the enclosure ceiling. The corresponding aperture ratios are $A_p = h/H = 1, \frac{3}{4}, \frac{1}{2}$, and $\frac{1}{4}$, respectively. All the partitions were 9.5 mm thick and traversed the full breadth of the enclosure in order to achieve, as nearly as possible, a two-dimensional system. Partitions which are effectively perfectly conducting are characterized by small temperature differences across the partition in comparison with the temperature difference ($T_h - T_c$), while effectively adiabatic partitions are characterized by negligible conduction heat transfer through the partition in comparison with the total energy transfer across the enclosure. A nondimensional partition conductance is defined by $k_p^* = (k_p/k)\,(L/\Delta x)/\mathrm{Nu}_L$, where Δx is the partition thickness. The criterion for a perfectly conducting partition is $k_p^* \gg 1$; for an adiabatic partition $k_p^* \ll 1$. In this experiment, the highly conducting partitions were fabricated from slabs of aluminum with $k_p^* \gtrsim 50$. The adiabatic partitions were made from polystyrene foam clad with 0.1 mm stainless steel sheets with $k_p^* \lesssim 0.02$.

To reduce energy losses to the surroundings, the entire apparatus was enclosed in a shell of polyurethane foam insulation, whose outer surface was covered with aluminum foil to reduce radiative losses.

The local surface temperatures of the hot and cold walls were determined with 30 gauge, copper-constantan thermocouples inserted in small holes which had been drilled horizontally into the hot and cold walls to a distance less than 1 mm from the inside (wet) surfaces of the hot and cold plates. Seventeen of these thermocouples were spread uniformly over each of the hot and cold walls.

The temperatures of the unheated surfaces (plexiglas floor and ceiling) were obtained with 50 gauge (0.025 mm dia), unsheathed, chromel-constantan thermocouples which were cemented to the plexiglas surface with a fine coating of polyurethane lacquer. The fine thermocouple wires ran perpendicular to the plane of Fig. 2 along the floor and ceiling. The thermocouple beads were located halfway between the two plexiglas endwalls at the positions $x/L = \frac{1}{4}, \frac{1}{2}$ and $\frac{3}{4}$. The very small diameter and the placement of the wires perpendicular to the plane of two-dimensionality minimized disturbance to the flow and axial conduction effects. The temperature at the lower edge of the partition, $y = h$, was measured with a fine, stainless-steel sheathed, chromel-constantan thermocouple probe with an overall dia of 0.25 mm. This sheathed thermocouple was also run perpendicular to the plane of Fig. 2, along the lower edge of the partition.

Local fluid temperatures within the enclosure were measured with thermocouple probe assemblies. Two fine, grounded junction, stainless-sheathed thermocouple probes (0.25 mm dia) were passed down through and out of a 1.6 mm dia stainless steel support tube, which was inserted vertically into the enclosure from the enclosure ceiling. The probe junctions were located about 6.5 cm from the larger support tube to minimize measurement errors due to the presence of the larger tube. Again, these fine probes were directed perpendicular to the plane of Fig. 2 to minimize heat conduction along the probe shafts. Three of these assemblies were used for measuring fluid temperature at the positions $x/L = \frac{1}{4}, \frac{1}{2}$ and $\frac{3}{4}$. Observations made during experiments both with and without the probes in place, revealed no detectable changes in either the flow or the overall heat transfer rate. Comparison of some of the thermocouples (both copper-constantan and chromel-constantan) with a precision mercury-in-glass thermometer showed that the standard calibration was adequate, with a maximum error of about ±1°C.

Energy input at the hot wall was measured with three single-element, electro dynamometer-type wattmeters, one for each power circuit, with accuracies of ± one percent. As a check on energy loss to the ambient, the heat transfer rate at the cold wall was measured and compared to the power input at the hot wall. Cooling water temperature entering and leaving the cold wall cooling manifold was mea-

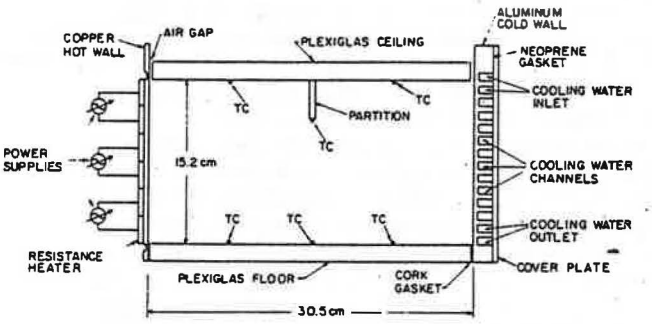

Fig. 2 Sketch of experimental apparatus

Nomenclature

$A = H/L$, aspect ratio
$A_p = h/H$, aperture ratio
B = enclosure breadth
c_p = constant pressure specific heat
g = acceleration due to gravity
H = enclosure height
h = distance from enclosure floor to partition
k = thermal conductivity
k_p = thermal conductivity of partition
k_p^* = nondimensional partition conductance
L = enclosure width
$\mathrm{Nu}_L = qL/(T_h - T_c)k$, Nusselt number
n = core temperature parameter
$\mathrm{Pr} = \frac{\nu}{\alpha}$, Prandtl number
$Q = (Q_h + Q_c)/2$, heat transfer across enclosure
Q_1 = heat transfer rate over lower third of hot wall
Q_2 = heat transfer rate over middle third of hot wall
Q_3 = heat transfer rate over upper third of hot wall
$q = Q/(B \cdot H)$, average heat flux
$\mathrm{Ra}_L = g\beta L^3(T_h - T_c)/\nu\alpha$, Rayleigh number
T = temperature
$T_r = (T_h + T_c)/2$, reference temperature
x = horizontal position coordinate
Δx = thickness of partial division
y = vertical position coordinate
α = thermal diffusivity
β = thermal coefficient of expansion
$\Lambda = \frac{k}{c_p}\left(\frac{\rho^2\beta}{\mu}\right)^{1/3}$ property group
μ = dynamic viscosity
ν = kinematic viscosity
ρ = density

Subscripts

c = cold wall
h = hot wall

sured with glass bead thermistors with a calibrated accuracy of ±0.05°C.

The procedure used in all of the experimental runs is as follows. The three heater circuits were used to heat the water to near-boiling temperature with the enclosure open to the atmosphere. Two to three hours at this temperature resulted in much of the dissolved gases being driven off. After the enclosure ceiling was inserted, the hot wall resistance heater power inputs were set and cooling water flow commenced. For the next four to five hours, adjustments were made in the relative power input to the three heater circuits to secure a reasonably isothermal condition on the hot wall. The cooling water flow rate was adjusted to limit temperature variations on the cold wall while still providing a moderate cooling water temperature increase (approximately 10°C). The wall temperatures T_h and T_c were taken as the average of the 17 temperatures measured on each of the hot and cold walls. Temperature variations from the mean wall temperature on the hot and cold walls seldom exceeded 10 percent of the overall temperature difference across the enclosure while the average deviation from the mean wall temperature was roughly three percent of $(T_h - T_c)$. There appeared to be no preferred direction for the wall temperature variation and observed local wall temperatures were very steady. The system was then allowed to equilibrate for an additional six hours. This extended beyond normal working hours in the laboratory so that perturbations in line voltage and cooling water flow rate and temperature were minimized.

The establishment of steady state conditions within the enclosure was a primary concern in the experimental procedure. Before any data were recorded, both cooling water inlet and exit temperature were carefully checked to insure that steady state conditions had been attained. This procedure was also repeated after the wall temperatures and fluid temperatures had been recorded. A sensitive check on the existence of steady state was provided by comparing the energy entering the enclosure at the hot wall, Q_h, to that leaving at the cold wall, Q_c. For all the experimental runs included in this study, these two rates of energy transfer differed by less than eight percent and in the great majority of cases the difference was less than five percent. These small fractional heat losses are a consequence of the large energy transfer rates occurring across the enclosure when water is the working fluid. For the total heat transfer across the enclosure, Q, required in determining the Nusselt number, the average of the heat transfer rates measured at the hot and cold walls was used, i.e., $Q = (Q_h + Q_c)/2$. Transport and thermodynamic properties for water were taken to be those at the reference temperature, $T_r = (T_h + T_c)/2$.

During many of the tests, an indication of the flow pattern within the enclosure was obtained by injecting dye into the flow. Roughly 0.5 cc of a dark blue dye was injected with a hypodermic syringe at the upper right-hand corner of the enclosure, midway between the two plexiglas endwalls. Observation of the subsequent dye motion was made through one of the endwalls and was enhanced by a white backdrop at the opposite endwall. The enclosure interior was illuminated by a photographic lamp mounted between the observer and the endwall observation window. The dye was injected and the dye front was allowed to progress a large distance from the point of injection before observations were made.

Results and Discussion

The laminar flow pattern observed in experiments for $A_p < 1$ is shown in Fig. 3. In general, for aperture ratios less than unity (i.e., when a partition was present), the flow was comprised of three relatively distinct regions. There was a peripheral, laminar boundary layer-type flow, a low velocity, relatively inactive core region, and a region of weak, clockwise recirculation in the upper left-hand quadrant of the enclosure. The peripheral flow was composed of thin, high-velocity boundary layers on the vertical surfaces with lower velocity, thicker layers (about 1 cm thickness) on the unheated horizontal surfaces. The boundary layer on the hot wall did not extend over the entire surface because most of the flow separated from the hot wall at approximately $y = h$ and then proceeded across the enclosure horizontally, in a thin, high-velocity layer until reaching the lower edge of the partition. The flow then, apparently without separating from the partition, turned upward along the cool side of the partition finally separating at a distance of one or two centimeters from the ceiling. In this region, the flow was observed to be somewhat unsteady, but the unsteadiness gradually disappeared as the fluid proceeded toward the top of the cold wall. The small amount of dye which entered the upper left quadrant of the enclosure allowed observation of the slowly recirculating flow there. The fraction of the flow entering this region was larger for conducting than for nonconducting partitions. The strength of the recirculating flow was also strongly dependent on the thermal boundary condition at the partition. Conducting partitions resulted in weak recirculation, while adiabatic partitions yielded either very weak or virtually no recirculation in that region. It is noted that in experiments with no partition (aperture ratio of unity) the recirculating region vanished, leaving only a large inactive central core and a peripheral boundary layer flow. It is very possible that interaction of the observed clockwise recirculating flow in the upper left hand quadrant and the high velocity layer at $y = h$ could have resulted in a multi-layer velocity profile in this region as in [21] via two counter-rotating vortices arranged vertically. However, in the vicinity of $y = h$, there was rather severe optical distortion due to the gradient in refractive index and the presumed lower, counterclockwise rotating vortex was not observed.

The flow pattern observed in the present high Ra_L experiments

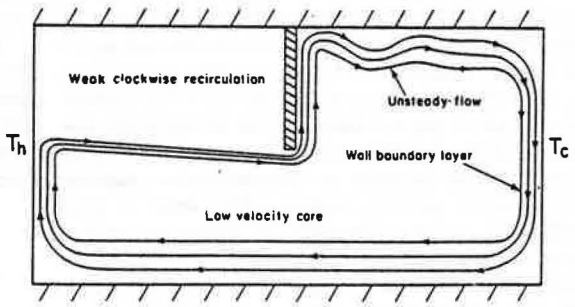

Fig. 3 Flow pattern observed in the cases of adiabatic and perfectly conducting partitions for $A_p < 1$ and $10^{10} \leqslant Ra_L \leqslant 10^{11}$

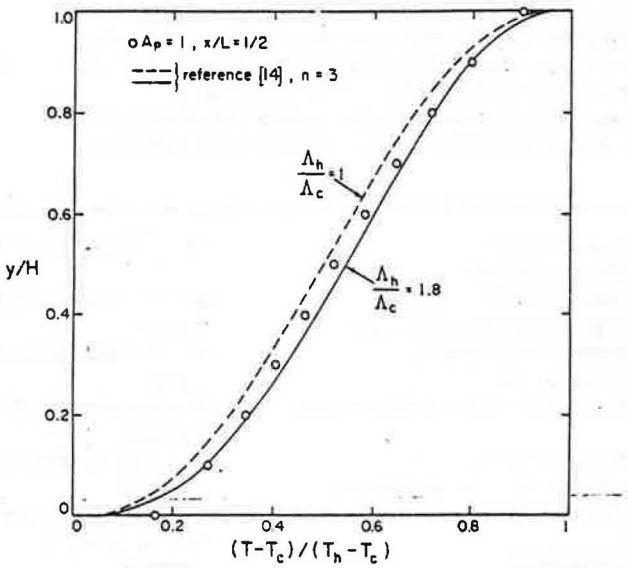

Fig. 4 Midslot vertical temperature profile in the undivided enclosure: $A = \frac{1}{2}$, $Ra_L = 6.41 \times 10^{10}$, $Pr = 3.7$, $T_h = 72°C$, $T_c = 25°C$

differed substantially from the flow pattern reported by Duxbury [20] in his partially divided enclosure with Ra_L approaching 10^6 and air ($Pr = 0.7$) as the working fluid. The flow visualization experiments of Duxbury show no distinct recirculating region and also little or no flow separation from the hot wall: two very prominent features of the high Ra_L experiments carried out in this study. Duxbury's experiments indicate some flow separation at the lower edge of the partition on the cool side. This may be due to the fact that in Duxbury's (lower Ra_L) experiments, the flow attempts to make a 180 deg turn as it passes the lower edge of the partition. Recall that in the high Ra_L experiments of this study, the flow only turns through an angle of about 90 deg because the main flow does not penetrate into the upper left quadrant of the enclosure. In general, the results of Duxbury indicate a much smaller inactive core region with thicker boundary layers.

From the flow visualization experiments, it was concluded that fully developed turbulent flow did not exist anywhere within the enclosure, even for Rayleigh numbers as high as 10^{11}. However, traveling wave-like motions, referred to by Elder [4] as "wall waves" were very prominent on both the heated and cooled vertical surfaces with no partition ($A_p = 1$). These waves, the first hint of transitional flow, developed at $y/H \simeq \frac{1}{3}$, and $y/H \simeq \frac{2}{3}$ on the hot and cold walls, respectively, and traveled in the same direction as the mean boundary layer flow. The waves, originally two-dimensional, traveled in a regular pattern up the hot wall and down the cold wall. Gradually, they developed three-dimensional characteristics and finally broke-up very near the upper left- and lower right-hand corners of the enclosure, so that a wave pattern could no longer be distinguished. In the experiments of Elder, with water in enclosures of aspect ratio, $10 \leq A \leq 30$ ($A = H/L$), the breaking up of the wall waves was accompanied by an intense wall layer-central core interaction. In the present experiments with $A = \frac{1}{2}$, very little, if any, interaction was observed. Perhaps the absence of this phenomena was due to the greater suppression of the interior flow by the horizontal walls for $A = \frac{1}{2}$. In the experiments with aperture ratio (A_p) less than unity (partial division present), the wall waves were indeed found to be significantly suppressed on both the hot and cold walls and completely absent on the hot wall for $y > h$.

A plot of the measured vertical temperature profile at $x/L = \frac{1}{2}$ for the case $A_p = 1$, i.e., no partition, is shown in Fig. 4. This profile exhibits the substantially linear, stable stratification in the enclosure core region which is a well-known characteristic of the boundary layer regime; see [2 and 16]. There is some asymmetry about the position $y/H = \frac{1}{2}$, which is probably due to the temperature dependence of the thermodynamic and transport properties of water. The dashed curve in Fig. 4 is the result of an approximate calculation of the core tem-

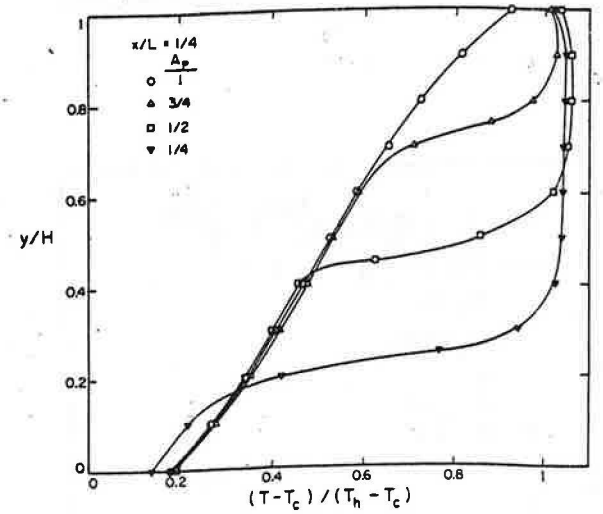

Fig. 5 Vertical temperature profiles at $x/L = \frac{1}{4}$, adiabatic partial divisions: $3.79 \times 10^{10} \leq Ra_L \leq 6.41 \times 10^{10}$, $3.7 \leq Pr \leq 4.2$

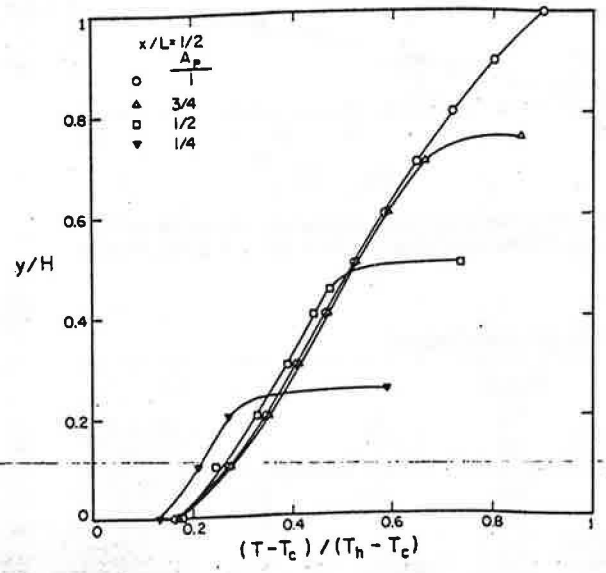

Fig. 6 Vertical temperature profiles at $x/L = \frac{1}{2}$ (in the aperture), adiabatic partial divisions: $3.79 \times 10^{10} \leq Ra_L \leq 6.41 \times 10^{10}$, $3.7 \leq Pr \leq 4.2$

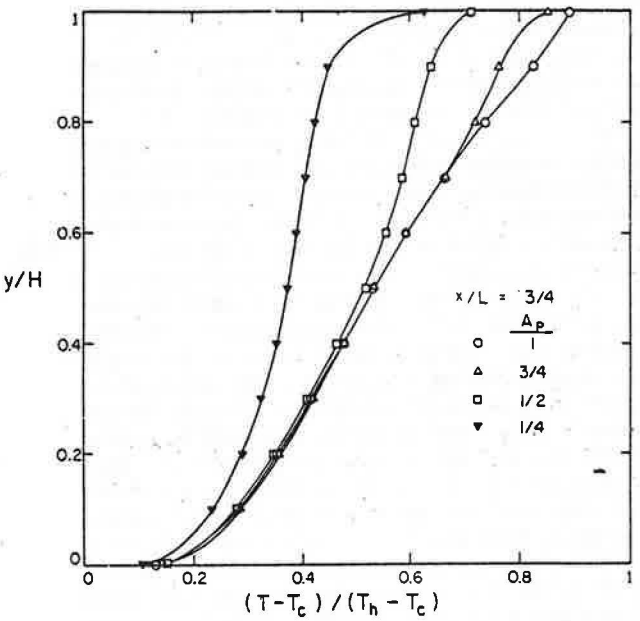

Fig. 7 Vertical temperature profiles at $x/L = \frac{3}{4}$, adiabatic partial divisions: $3.79 \times 10^{10} \leq Ra_L \leq 6.41 \times 10^{10}$, $3.7 \leq Pr \leq 4.2$

Table 1 Local heat transfer rates corresponding to Figs. 4–7

A_p	$Q_1(W)$ (Q_1/Q_h)	$Q_2(W)$ (Q_2/Q_h)	$Q_3(W)$ (Q_3/Q_h)	$Q_h(W)$
$\frac{1}{4}$	880 (0.965)	32 (0.035)	0 (0.0)	912
$\frac{1}{2}$	1020 (0.761)	288 (0.215)	32 (0.024)	1340
$\frac{3}{4}$	897 (0.627)	418 (0.292)	115 (0.080)	1430
1	1430 (0.559)	756 (0.295)	373 (0.146)	2559

perature distribution due to Raithby, et al. [14] for enclosures of aspect ratio, $A \gtrsim 5$, filled with a constant property fluid; that is $\Lambda_h = \Lambda_c$, where the property group,

$$\Lambda = \frac{k}{c_p}(\rho^2 \beta/\mu)^{1/3}. \quad (1)$$

Because the mid-cavity temperature gradient, $\partial[(T - T_c)/(T_h - T_c)]/\partial(y/H)$, at $x = L/2$, $y = H/2$, was measured to be 0.59, the Prandtl number-dependent parameter, n, of reference [14] was given a numerical value of 3.0 in generating the curves of Fig. 4 as suggested by Raithby, et al. [14]. The solid curve in Fig. 4 represents the result for the core temperature from [14] for $\Lambda_h/\Lambda_c = 1.8$ which corresponds to the actual wall temperatures ($T_h = 72°C$, $T_c = 25°C$) for the plotted data. Both core temperature predictions yield reasonably good estimates of the measured core temperature; the variable property calculation giving slightly better agreement. Apparently, the calculation technique of Raithby, et al. may be applied with some confidence even somewhat beyond its supposed range of validity ($A \gtrsim 5$).

Vertical temperature profiles at the positions $x/L = \frac{1}{4}, \frac{1}{2}$, and $\frac{3}{4}$ are plotted in Figs. 5, 6, and 7, respectively for the case of $k_p^* \ll 1$ (adiabatic partitions). All the data in these figures were taken in the Ra_L range, $10^{10} \leq Ra_L \leq 10^{11}$. Over this range it was found that for fixed A_p the non-dimensional temperature profiles are virtually independent of the Rayleigh number. It should be pointed out that no attempt was made to measure the temperature distribution in the thin boundary layers adjacent to the enclosure floor and ceiling. Detailed numerical computations for the case, $A_p = 1$, have shown that for large Ra_L the temperature gradient at the adiabatic surfaces approaches zero only in a very small region near the surface [9]. Measurements were not made in this region and therefore the data often exhibit an apparent non-zero gradient at $y/H = 0$ and 1. Note also that for aperture ratios of $\frac{3}{4}$ and $\frac{1}{2}$ the temperature profiles at each x position are very close to the profiles measured with no partial division ($A_p = 1$) for values of $y/H \lesssim A_p$. This indicates that for aperture ratios at least as small as $\frac{1}{2}$ the temperature field in the lower two quadrants of the partially divided enclosure is substantially unaffected by the partial division. However, for $A_p = \frac{1}{4}$ the partial division apparently has the effect of causing a small temperature decrease for $y/H \lesssim A_p$.

The profiles measured at $x/L = \frac{1}{4}$ (see Fig. (5)) exhibit a small region near $y/H = A_p$, where the temperature increases rapidly to the average hot wall temperature, T_h. The temperature then remains very nearly constant for elevations greater than $y \simeq h$. It was in this region of large temperature gradient that small temperature fluctuations, of the order of $\frac{1}{4}°C$, were detected during the experiments. The time scale, however, of the fluctuations could not be properly investigated due to the long response time of the measurement system. The finite temperature gradient at $y = H$ in Fig. 5 is probably indicative of a small conduction heat loss through the enclosure ceiling since very little or no convection occurs in this region. Also, note in Fig. 5 that the temperature in the upper left quadrant slightly exceeds the average hot wall temperature, T_h. The profiles measured at $x/L = \frac{1}{2}$ (in the aperture plane), Fig. 6, show a very rapid temperature increase in the region close to $y/H = A_p$. It is again emphasized (referring to Fig. 6) that the partial division seems to have little effect on the temperature below $y \simeq h$ except for aperture ratios approaching $\frac{1}{2}$.

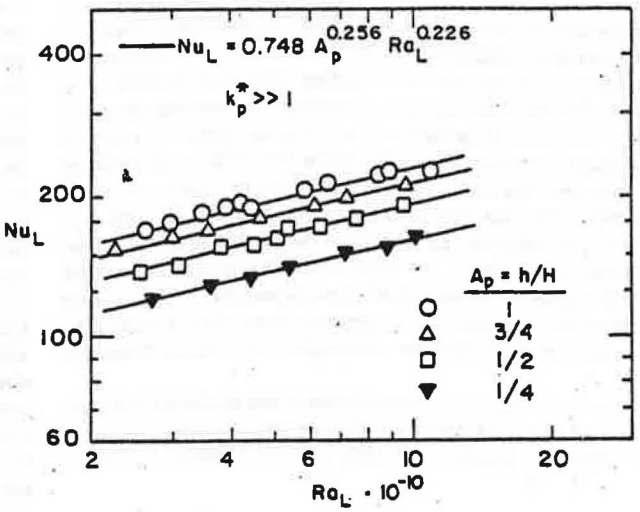

Fig. 8 Heat transfer results and correlation for conducting partial divisions: $3.0 \leq Pr \leq 4.3$

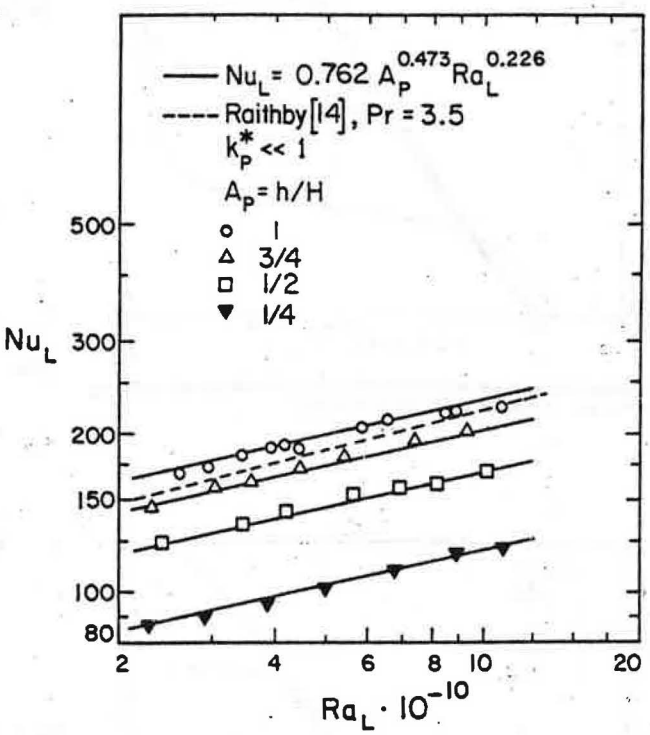

Fig. 9 Heat transfer results and correlation for adiabatic partial divisions: $3.0 \leq Pr \leq 4.3$, Raithby correlation with $Pr = 3.5$, $A = \frac{1}{2}$, $Nu_L = 0.392\ Ra_L^{1/4}$

Table 2 Data for the case $A_p = \frac{1}{2}$, adiabatic partial division

Run	$Ra_L \cdot 10^{-10}$	Pr	Nu_L	Q_h (W)	Q_c (W)	$\frac{Q_h - Q_c}{Q_h}$ (%)	T_h (°C)	T_c (°C)	$T_h - T_c$ (°C)
1	4.21	3.8	142	1290	1260	2.3	63.0	29.6	33.4
2	5.65	3.6	153	1680	1640	2.4	69.8	29.7	40.1
3	3.46	3.9	135	1050	1020	2.9	59.4	30.8	28.6
4	2.41	4.4	125	820	780	4.9	51.4	27.1	24.3
5	6.94	3.4	157	1940	1930	0.5	75.2	29.6	45.6
6	8.19	3.3	161	2220	2210	0.5	79.8	29.2	50.6
7	10.2	3.1	170	2640	2580	2.3	86.5	30.3	56.2

The effect of the partial divisions at $x/L = \frac{3}{4}$ (Fig. 7) is to decrease the temperature for $y/H \gtrsim A_p$, the effect becoming stronger with decreasing aperture ratio. This behavior seems reasonable because for a non-conducting partition as aperture ratio approaches zero: i.e., the completely divided enclosure, $T \to T_h$ for $x < L/2$ and $T \to T_c$ for $x > L/2$.

In general, the measured temperature profiles seem to verify the statements made concerning the basic nature of the flow in the partially divided enclosure: i.e., the existence of an inactive core region, a region of very weak recirculation and a peripheral boundary-layer flow.

Local hot wall heat transfer rates for experiments with and without adiabatic partial divisions are shown in table 1. (In this table, Q_1 represents the heat transfer rate over the lower one-third of the hot wall, while Q_2 and Q_3 are the rates for the middle and upper one-third, respectively.) The results of the seven heat transfer experiments for $A_p = \frac{1}{2}$ and $k_p^* \ll 1$ are listed in table 2. In all of the experiments the wall temperature difference was greater than 22°C but never exceeded 61°C. The heat transfer data for conducting and non-conducting partitions are presented graphically in Figs. 8 and 9. Note that in Fig. 9 the approximate Nusselt number prediction of Raithby, et al. [14] for undivided enclosures ($A_p = 1$) in the laminar boundary layer regime again gives a reasonably good estimate of the heat transfer in the enclosure of aspect ratio $A = \frac{1}{2}$, even though this prediction was generated on the basis of rather tall, narrow enclosures: i.e., vertical layers with $A \gtrsim 5$. From the data in Figs. 8 and 9 the following correlations were generated for the cases of conducting and non-conducting partial divisions:

$$\mathrm{Nu}_L = 0.748\, A_p^{0.256}\, \mathrm{Ra}_L^{0.226} \quad \text{(conducting partitions)} \qquad (2)$$

$$\mathrm{Nu}_L = 0.762\, A_p^{0.473}\, \mathrm{Ra}_L^{0.226} \quad \text{(non-conducting partitions)} \qquad (3)$$

where the root-mean-square deviation of the data from the correlations are 2.5 and 3.8 for conducting and non-conducting partitions, respectively. Note from Figs. 8 and 9 that there is virtually no difference in the Rayleigh number dependence of the Nusselt number as A_p is varied, that is, all curves have roughly the same slope regardless of the aperture ratio. This behavior was also found at a lower Ra_L, with air [20]. Also note that the heat transfer dependence on A_p increases substantially (the exponent of A_p in equations (2) and (3) changes approximately from $\frac{1}{4}$ to $\frac{1}{2}$) when the enclosure is partially divided by a non-conducting rather than by a conducting partition. This increased dependence on A_p supports the earlier observation that the flow recirculation in the upper left-hand quadrant of the partially divided enclosure is severely limited by non-conducting partition materials. Thus, adiabatic partitions represent an increased resistance to the heat transfer across the enclosure with a greater resulting sensitivity to the aperture ratio.

It is noted that the above cited results for the dependence of the heat transfer on A_p do not agree with the results of the low Rayleigh number experiments with air [20]. Duxbury's data for enclosures of aspect ratio, $A = \frac{8}{3}$, with conducting partitions, are found to be reasonably well correlated by a relation of the form given by equation (2) with an aperture ratio dependence of $A_p^{0.41}$ rather than $A_p^{0.256}$ as was found in this study. However, this discrepancy is not too surprising since the two experiments were carried out at different values of Pr (0.7 in [20] versus 3.5 for this study) and at widely different values of Ra_L (10^6 versus 10^{10}). In addition, it is believed that the substantial heat losses (15–40 percent) from the experimental cells of Duxbury may have adversely effected the accuracy of his results.

Conclusions

Experiments with water in a partially divided rectangular enclosure have revealed the existence of three relatively distinct regions at Rayleigh numbers approaching 10^{11}: i.e. the existence of an inactive core region, a region of very weak recirculation and a peripheral boundary-layer flow. The partial divisions were also shown to significantly decrease the overall heat transfer, especially when the partitions were non-conducting. Also, laminar-transitional flow on the enclosure vertical surfaces was found to be suppressed markedly by the presence of the divisions. These results could be significant with respect to design considerations in solar heating applications.

It is recommended that further study be directed toward the determination of the separate effects of Prandtl number and aspect ratio on the heat transfer. It is not clear, for example, how much of the discrepancy found between Duxbury's results and the present results is due to differences in Ra_L (10^6 versus 10^{10}) or due to differences in Pr (0.7 versus 3.5). Extending the range of Ra_L to larger values should also serve to expose the role of partial divisions in retarding the transition to turbulent flow, a subject which has only been alluded to in the present work. Finally, a more detailed accounting of the local fluid velocities within the enclosure would be instrumental in gaining an understanding of the rather complex flow observed in these experiments.

Acknowledgement

This work has been supported in part by the Research and Development Branch, Passive and Hybrid Division, of the Office of Solar Applications for Buildings, U.S. Department of Energy, under Contract No. W-7405-ENG-48. The authors also wish to acknowledge Fred Bauman of the Lawrence Berkeley Laboratory for his assistance during the early stages of this research.

References

1 Batchelor, G. K., "Heat Transfer by Free Convection Across a Closed Cavity Between Vertical Boundaries at Different Temperatures," *Quart. of Applied Mathematics*, Vol. XII, 1954, pp. 209–233.

2 Eckert, E. R. G. and Carlson, W. D., "Natural Convection in an Air Layer Enclosed Between Two Vertical Plates with Different Temperatures," *International Journal of Heat Mass Transfer*, Vol. 2, 1961, pp. 106–120.

3 Dropkin, D. and Somerscales, E., "Heat Transfer by Natural Convection in Liquids Confined by Two Parallel Plates Which are Inclined at Various Angles with Respect to the Horizontal," JOURNAL OF HEAT TRANSFER, Vol. 87, 1965, pp. 77–84.

4 Elder, J. W., "Turbulent Free Convection in a Vertical Slot," *Journal of Fluid Mechanics*, Vol. 23, 1965, pp. 99–111.

5 Emery, A. and Chu, N. C., "Heat Transfer Across Vertical Layers," JOURNAL OF HEAT TRANSFER, Vol. 87, 1965, pp. 110–116.

6 de Vahl Davis, G., "Laminar Natural Convection in an Enclosed Rectangular Cavity," *International Journal of Heat and Mass Transfer*, Vol. 11, 1968, pp 1675–1693.

7 Torrance, K. E., "Comparison of Finite-Difference Computations of Natural Convection," *Journal of Research of the National Bureau of Standards, B. Mathematical Sciences*, Vol. 72B, 1968, pp. 281–301.

8 Mac Gregor, R. K. and Emery, A. F., "Free Convection through Vertical Plane Layers, Moderate and High Prandtl Number Fluids," JOURNAL OF HEAT TRANSFER, Vol. 91, 1969, pp. 391–403.

9 Rubel, R. and Landis, F., "Numerical Study of Natural Convection in a Vertical Rectangular Enclosure," *Physics of Fluids Supplement II*, Vol. 12, 1969, pp. 203–213.

10 Newell, M. E. and Schmidt, F. W., "Heat Transfer by Laminar Natural Convection within Rectangular Enclosures," JOURNAL OF HEAT TRANSFER, Vol. 92, 1970, pp. 159–165.

11 Ostrach, S., "Natural Convection in Enclosures," *Advances in Heat Transfer*, Academic Press, Vol. 8, 1972, pp. 161–227.

12 Raithby, G. D. and Hollands, K. G. T., "A General Method of Obtaining Approximate Solutions to Laminar and Turbulent Free Convection Problems," *Advances in Heat Transfer*, Academic Press, Vol. 11, 1975, pp. 265–315.

13 Arnold, J. N., Catton, I. and Edwards, D. K., "Experimental Investigation of Natural Convection in Inclined Rectangular Regions of Differing Aspect Ratios," JOURNAL OF HEAT TRANSFER, Vol. 98, 1976, pp. 67–71.

14 Raithby, G. D., Hollands, K. G. T. and Unny, T. E., "Analysis of Heat Transfer by Natural Convection Across Vertical Fluid Layers," JOURNAL OF HEAT TRANSFER, Vol. 99, 1977, pp. 287–293.

15 Sernas, V. and Lee, E. I., "Heat Transfer in Air Enclosures of Aspect Ratio Less than One," ASME 78-WA/HT-7, 1978.

16 Lee, E. I. and Sernas, V., "Numerical Study of Heat Transfer in Rectangular Air Enclosures of Aspect Ratio Less Than One," ASME 80-WA/HT-45, 1980.

17 Bauman, F., Gadgil, A., Kammerud, R. and Greif, R. "Buoyancy Driven Convection in Rectangular Enclosures: Experimental Results and Numerical Calculations," ASME 80-HT-66, 1980.

18 ElSherbiny, S. M., Raithby, G. D., and Hollands, K. G. T., "Heat Transfer by Natural Convection Across Vertical and Inclined Air Layers," ASME 80-HT-67, 1980.

19 LeQuere, P., Humphrey, J. A. C. and Sherman, F. S., "Numerical Calculation of Thermally Driven Two-Dimensional Unsteady Laminar Flow in Cavities of Rectangular Cross-Section," University of California, Berkeley,

Report No. FM 80/1, 1980.

20 Duxbury, D., "An Interferometric Study of Natural Convection in Enclosed Plane Air Layers with Complete and Partial Central Vertical Divisions," Ph.D. thesis, University of Salford, 1979.

21 Lynch, N. P., and Lloyd, J. R., "An Experimental Investigation of the Transient Build-Up of Fire in a Room Corridor Geometry," *18th International Symposium on Combustion*, The Combustion Institute, Pittsburgh, Pa., 1980.

22 Ku, A. C., Doria, M. L. and Lloyd, J. R., "Numerical Modeling of Unsteady Buoyant Flows Generated by Fire in a Corridor," *16th International Symposium on Combustion*, The Combustion Institute, Pittsburgh, Pa., 1976, pp. 1373–1384.

23 Janikowski, H. E., Ward, J. and Probert, S. D., "Free Convection in Vertical Air-Filled Rectangular Cavities Fitted with Baffles," *6th International Heat Transfer Conference*, Toronto, Vol. 2, pp. 257–262.

24 Emery, A. F., "Exploratory Studies of Free Convection Heat Transfer Through an Enclosed Vertical Liquid Layer with a Vertical Baffle," JOURNAL OF HEAT TRANSFER, Vol. 91, 1969, pp. 163–165.

25 Bejan, A., and Tien, C. L., "Laminar Natural Convection Heat Transfer in a Horizontal Cavity with Different End Temperatures," JOURNAL OF HEAT TRANSFER, Vol. 100, 1978, pp. 641–647.

TECHNICAL NOTES

DISCUSSION